Research Square

Preprints are preliminary reports that have not undergone peer review.
They should not be considered conclusive, used to inform clinical practice,
or referenced by the media as validated information.

Molecular docking and pharmacokinetic studies of bioactive compounds from medicinal plants as promising inhibitory agents against Mycobacterium tuberculosis Enoyl-acyl carrier protein (ACP)-reductase (InhA)

Oluwasegun O. Fawibe
fawibeoo@funaab.edu.ng
Federal University of Agriculture Abeokuta
Bolanle R. Lawal
Federal University of Agriculture Abeokuta
Abdulwakiil A. Mustafa
Federal University of Agriculture Abeokuta
Abidemi O. Bankole
Federal University of Agriculture Abeokuta
Samuel A. Poku
University of Ghana

Research Article

Keywords: Molecular docking, medicinal plants, phytochemicals, tuberculosis, drug development

Posted Date: November 28th, 2023

DOI: https://doi.org/10.21203/rs.3.rs-3654525/v1

License: This work is licensed under a Creative Commons Attribution 4.0 International License. Read Full License

Additional Declarations: No competing interests reported.

Version of Record: A version of this preprint was published at In Silico Pharmacology on November 14th, 2025. See the published version at https://doi.org/10.1007/s40203-025-00472-9.

Abstract

Tuberculosis (TB) is a significant global public health challenge. Targeting enoyl-acyl carrier protein (ACP) reductase (InhA), an enzyme involved in mycolic acid biosynthesis, is a promising path to discovering an effective treatment for tuberculosis. This study assessed the inhibitory potential of bioactive compounds from four medicinal plants (*Garcinia kola*, *Moringa oleifera*, *Newbouldia laevis*, and *Ocimum gratissimum*) and control drugs (Isoniazid and Ethionamide) against InhA. Molecular docking and computational tools were used to evaluate the binding affinities and interactions with InhA's active site. Drug-likeness, binding affinities, bioactivity, and absorption, distribution, metabolism, excretion, and toxicity (ADMET) attributes were determined using online tools. Ten out of twenty-three bioactive compounds studied were screened out due to their violation of Lipinski's, Ghose's, Veber's, Egan's, or Muegge's rules. Interestingly, the remaining thirteen compounds showed stronger binding affinities with InhA than those of the control drugs, depicting them as potential anti-tuberculosis drugs. The binding energy of the bioactive compounds ranged from − 8.0 to -9.5 kcal/mol while those of Isoniazid and Ethionamide, were 6.1 kcal/mol and − 6.0 kcal/mol, respectively. Also, the compounds exhibited hydrogen bonds, hydrophobic, and π stacking interactions with the active site residues of the protein; hence, contributing to their potential as antituberculosis agents. The ADMET property of each of the hit ligands predicted its ability to effectively reach and remain at the target protein to exert its therapeutic influence. The study depicts that the screened bioactive compounds exhibited more favorable docking interactions with the target protein than the control drugs, potentially contributing to tuberculosis treatment.

INTRODUCTION

Tuberculosis (TB), a disease caused by *Mycobacterium tuberculosis* (M.tb), is an ancient and contagious epidemic that primarily affects the lungs but can also spread to the brain and spinal cord. Despite being both preventable and treatable, it resulted in the loss of 1.6 million lives in 2021, including 187,000 individuals who were co-infected with HIV (Natarajan et al. 2020 and WHO, 2023). Globally, TB ranks as the 13th leading cause of death and is the second most deadly infectious disease after COVID-19. In 2021, 10.6 million people were infected with TB, with the majority of cases occurring in low and middle-income countries, particularly in nations such as Nigeria, Pakistan, the Philippines, Bangladesh, China, India, Indonesia, and South Africa (WHO, 2023).

TB has contributed significantly to the development of antibiotics. However, concerns are mounting among experts due to the resurgence of TB as a public health threat which primarily stems from the emergence of drug-resistant strains of *M. tuberculosis* (Jagadeb et al. 2019). The development of these strains has been linked to inappropriate usage of TB medications, including incorrect prescriptions, substandard drug quality, and premature treatment discontinuation (WHO, 2023). The resistant nature of TB has resulted in further classifications such as multi-drug-resistant (MDR), extensively drug-resistant (XDR) (Espinal, 2003), and totally drug-resistant (TDR) (Velayati et al. 2013) tuberculosis. These strains of TB show resistance to anti-TB drugs such as ethionamide, isoniazid, ethambutol, rifampicin, and pyrazinamide (Farjallah et al. 2021). Moreover, the coinfection of TB with HIV/AIDS has further exacerbated this issue (Morrison et al. 2008).

A key enzyme in the *Mycobacterium tuberculosis* (Mtb) pathway, enoyl-acyl carrier protein (ACP) reductase (InhA) has been identified as a promising target for TB drug development (Jayaraman et al. 2021). InhA catalyzes the β-nicotinamide adenine dinucleotide (NADH)-specific reduction of fatty acid precursors. Its role is also crucial to the biosynthesis of mycolic acids, and other vital components of the mycobacterial cell wall (Massengo-Tiasse et al. 2009). Blocking InhA disrupts the cell wall's integrity and kills the bacterium. This mechanism underlies the development of frontline anti-TB drugs such as isoniazid (Kamsri et al. 2019), highlighting InhA's significance as a therapeutic target protein. Despite drug resistance, challenges, and adverse effects linked to existing TB treatments, there is a growing interest in exploring natural products, particularly those derived from medicinal plants, as potential sources of new anti-TB agents. Multi-drug resistance has rapidly emerged in clinical practice, highlighting the narrow window for new drug effectiveness. This underscores the urgent need for rapid drug development and continuous research efforts. Novel, potent, and safer anti-TB drugs are required to counter acquired resistance and shorten lengthy drug regimens.

Medicinal plants offer an alternative to conventional drugs for TB treatment. These plants, serving as natural resources have played essential cultural roles and continue to be integral to human lifestyles (Pakadang et al. 2021). Furthermore, these plants form the basis for new drug and pharmaceutical product development (Samje et al. 2021). Many contain bioactive compounds that contribute to ailment prevention and treatment by promoting antioxidant activity, inhibiting microbial growth, and influencing genetic pathways. Notably, there has been a growing global interest in the use of plant-based secondary metabolites for the treatments of various human ailments compared to the use of synthetic drugs, mainly due to their cost-effectiveness, widespread availability, and limited adverse effects. In recent times, pharmacologically effective medications with minimal or no adverse effects have been derived from natural origins, especially microbes and medicinal plants (Atanasov et al. 2015). Moreover, certain plant-derived bioactive compounds exhibit antibacterial properties, making them potential sources for the derivation of bioactive agents against Mtb.

Garcinia kola, a flowering plant in the Mangosteen genus, is utilized in traditional medicine for treating various ailments including bacterial infection. Notably, *Garcinia kola* seeds and bark are valued for their medicinal properties (Emmanuel et al. 2022). The plant contains compounds such as kolaviron with potential drug discovery applications (Buba et al. 2016). In vivo and in vitro pharmacological studies have unveiled a spectrum of benefits associated with *G. kola*, including antimalarial, anti-inflammatory, anti-asthmatic, neuroprotective, antidiabetic activities, hepatoprotective, and antioxidant (Buba et al. 2016; Emmanuel et al. 2022). Also, *Moringa oleifera* is a versatile tree with widespread use in food, medicine, and water purification (Zaku et al. 2015). Rich in phytochemicals, it exhibits numerous pharmacological properties, including antimicrobial, hypotensive, and immunomodulatory effects (Bhattacharya et al. 2018). The plant's antimicrobial potential has been explored, specifically against *Salmonella* spp and *M. tuberculosis*. Its diverse applications make it a valuable asset in both health and medicine (Ugboko et al. 2020). *Newbouldia laevis* is another tropical African angiosperm used to mark property boundaries. Its folk medicinal use is attributed to specific chemical substances (Dermane et al. 2020). Kuete et al. (2007) identified ten compounds in its root bark extract with potent antimicrobial properties. Other studies found furanonaphthoquinones and benzofuran derivatives (Gormann et al. 2003). Alkaloids, saponins, flavonoids, and more are consistently detected in *N. laevis* extracts (Anaduaka et al. 2013). This highlights the plant's potential medicinal value due to its bioactive compounds, especially in microbial treatment. *Ocimum gratissimum* known as clove basil or African basil, is a fragrant basil species. Native

to Africa and Asia, it's used for culinary and medicinal purposes (Mohr et al. 2017; Ugbogu et al. 2021). It is rich in macronutrients and offers nutritional value. It possesses antimicrobial properties, with its essential oil used for preservation and antioxidant effects.

Molecular docking has become a predictive modeling technique that can elucidate the interactions between receptor proteins and bioactive compounds, hence, providing information on their mechanisms and interaction (Jakhar et al. 2020). In silico identification of potential hit ligands has gained popularity in computer-aided drug discovery (Kazmi et al. 2019). This approach streamlines the search for lead compounds from extensive databases and facilitates understanding potential hits compounds' mechanisms aiding bioactivity optimization. This study employs an in-silico analysis to evaluate bioactive compounds in selected medicinal plants (*Garcinia kola*, *Newbouldia laevis*, *Ocimum gratissimum*, and *Moringa oleifera)* capable of inhibiting enoyl-acyl carrier protein (ACP) reductase (InhA). The study also assesses the drug-likeness and pharmacokinetics of these bioactive compounds.

MATERIALS AND METHODS

Ligand Selections

Twenty-four (23) bioactive compounds were selected from four different plants (*Garcinia kola*, *Newbouldia laevis*, *Ocimum gratissimum*, and *Moringa oleifera).* Garcifuran B, Cycloartenol, 2-Hydroxyxanthone, 1,5-Dihydroxyxanthone, 3-hydroxy-4-methoxyxanthone, and 1,2-dimethoxyxanthone were selected from *G. kola* (Tauchen et al. 2023); Galactose, Tocopherols, Rhamnetin, Isoquercitrin, and Kaempferitrin from *M. oleifera* (Padayachee et al. 2020); Napabucasin, Beta-Lapachone, Lapachol, and 5,7-Dihydroxydehydroiso-α-lapachone from *N. laevis* (Dermane et al. 2020); while, 1,8-Cineole, Eugenol, Quercetin, Kaempferol, Catechin, Nepetrin, Rutin, and Terpinen-4-ol were selected from *O. gratissimum* (Edo et al. 2023 and Melo et al. 2019), Isoniazid and Ethionamide were selected as control drugs with inhibitory activities against InhA. PubChem identification numbers (PIDs), 3D structures in structure data format (SDF), and canonical SMILES of the bioactive compounds and those of the control drugs were retrieved from PubChem Web https://pubchem.ncbi.nlm.nih.gov/compound/ (Table 1).

Table 1
Library of selected plants, compounds and their canonical smile

S/N	Plant	Name Of Compound	ID	Canonical Smile
1	*Garcinia kola*	Garcifuran B	11780117	COC1 = CC(= CC(= C1O)O)C2 = CC3 = C(C = C2)OC = C3
2		Cycloartenol	92110	CC(CCC = C(C)C)C1CCC2(C1(CCC34C2CCC5C3(C4)CCC(C5(C)C)O)O)C)C
3		2-Hydroxyxanthone	74708	C1 = CC = C2C(= C1)C(= O)C3 = C(O2)C = CC(= C3)O
4		1,5-Dihydroxyxanthone	5480299	C1 = CC2 = C(C(= C1)O)OC3 = CC = CC(= C3C2 = O)O
5		3-Hydroxy-4-methoxyxanthone	5464639	COC1 = C(C = CC2 = C1OC3 = CC = CC = C3C2 = O)O
6		1,2-Dimethoxyxanthone	14189053	COC1 = C(C2 = C(C = C1)OC3 = CC = CC = C3C2 = O)OC
7	*Moringa oleifera*	Galactose	6036	C(C1C(C(C(C(O1)O)O)O)O)O)O
8		Tocopherols	14986	CC1 = C(C = C2CCC(OC2 = C1C)(C)CCCC(C)CCCC(C)CCCC(C)C)O
9		Rhamnetin	5281691	COC1 = CC(= C2C(= C1)OC(= C(C2 = O)O)C3 = CC(= C(C = C3)O)O)O
10		Isoquercitrin	5281643	C1 = CC(= C(C = C1C2 = C(C(= O)C3 = C(C = C(C = C3O2)O)O)OC4C(C(C(C(O4)CO)O)O)O)O)O
11		Kaempferitrin	5486199	CC1C(C(C(C(O1)OC2 = CC(= C3C(= C2)OC(= C(C3 = O)OC4C(C(C(C(O4)C)O)O)O)C5 = CC = C(C = C5)O)O)O)O)O
12	*Newbouldia laevis*	Napabucasin	10331844	CC(= O)C1 = CC2 = C(O1)C(= O)C3 = CC = CC = C3C2 = O
13		Beta-Lapachone	3885	CC1(CCC2 = C(O1)C3 = CC = CC = C3C(= O)C2 = O)C
14		Lapachol	3884	CC(= CCC1 = C(C2 = CC = CC = C2C(= O)C1 = O)O)C
15		5,7-Dihydroxydehydroiso- α-Lapachone	10802099	CC(= C)C1CC2 = C(O1)C(= O)C3 = C(C2 = O)C(= CC(= C3)O)O
16	*Ocimum gratissimum*	1,8-Cineole	2758	CC1(C2CCC(O1)(CC2)C)C
17		Eugenol	3314	COC1 = C(C = CC(= C1)CC = C)O
18		Quercetin	5280343	C1 = CC(= C(C = C1C2 = C(C(= O)C3 = C(C = C(C = C3O2)O)O)O)O)O)O
19		Kaempferol	5280863	C1 = CC(= CC = C1C2 = C(C(= O)C3 = C(C = C(C = C3O2)O)O)O)O
20		Catechin	9064	C1C(C(OC2 = CC(= CC(= C21)O)O)C3 = CC(= C(C = C3)O)O)O
21		Nepetrin	120742	COC1 = C(C = C2C(= C1O)C(= O)C = C(O2)C3 = CC(= C(C = C3)O)O)OC4C(C(C(C(O4)CO)O)O)O
22		Rutin	5280805	CC1C(C(C(C(O1)OCC2C(C(C(C(O2)OC3 = C(OC4 = CC(= CC(= C4C3 = O)O)O)C5 = CC(= C(C = C5)O)O)O)O)O)O)O)O
23		Terpinen-4-Ol	11230	CC1 = CCC(CC1)(C(C)C)O
24	Control drugs	Isoniazid (INH)	3767	C1 = CN = CC = C1C(= O)NN
25		Ethionamide (ETH)	2761171	CCC1 = NC = CC(= C1)C(= S)N

Protein targets selection and preparation

Enoyl-acyl carrier protein (ACP) reductase, known as InhA, was selected as the target protein (Hazbon et al. 2006). The three-dimensional (3D) crystallographic structure of the target protein (PDB: 1BVR) (Rozwarski et al. 1999) was retrieved from the Research Collaboratory for Structural Bioinformatics (RCSB) Protein Data Bank (www.rcsb.org) (Berman et al. 2000) and subsequently saved in PDB format (Fig. 1).

The UCSF Chimera (version 1.13.1) was used for the separation of the 3D structure of the target protein (InhA) from co-crystallized ligands (Pettersen, 2004). Additionally, UCSF Chimera was employed for the removal of water, hydrogen addition, and Gasteiger-Hückel charge assignment in preparation for molecular docking.

Drug likeness screening

With the use of canonical SMILES, twenty-four (23) bioactive compounds and two (2) control drugs were screened for drug-likeness properties using the online server SwissADME (http://swissadme.ch/) (Daina et al. 2017). The bioactive compounds were screened using Lipinski, Ghose, Veber, Egan, and Muegge rules (Lipinski, 2016; Bickerton et al. 2012; Veber et al. 2002; Egan et al. 2000; Muegge et al. 2001). Except for the control drugs, bioactive compounds with any violation of the rules were eliminated and not considered for further studies. However, compounds with no violation were subjected to molecular docking and further analysis.

Ligand optimization and molecular docking

The molecular docking of the bioactive compounds with InhA was conducted using the Python Prescription (PyRx) (version 0.8) software (Trott and Olson, 2010). The 3D structures of the ligands were uploaded to Open Babel, while optimization of the ligands to their lowest energy states for docking was carried out using the Merck Molecular Force Field (MMFF94) and afterward converted into the AutoDock ligand format (PDBQT). Moreover, the molecular docking of the ligands to the protein receptors was conducted using AutoDock Vina. To define the proteins' active site, a grid box with the following dimensions was employed: center (x: 17.1892, y: 7.5962, z: 14.2580), size (x: 64.8333, y: 69.4574, z: 71.8294 angstroms) and an exhaustiveness level of 10 was selected for the molecular docking process. The resulting binding energy for each ligand and its interaction with the protein was recorded in kcal/mol. The PDBQT format of the docked ligands and the target protein was converted to PDB format using PyRx, and saved for further evaluation and visualization.

Binding site prediction and molecular interaction analysis

The binding and potential allosteric sites were analyzed and identified using the PockDrug-server. Binding pockets with favorable energetic properties were identified using van der Waals probes embedded in the web. Also, the top-ranked possible receptor sites with residue numbers ranging from 9 to 44 were identified using PockDrug-server (Fig. 2). The favorable receptor sites were selected based on factors such as site score, druggability score, and size (Hussein et al. 2015).

To analyze the interactions between the ligands and the target protein, protein-ligand complexes were created using PyMOL© molecular graphics software (version 2.4, 2010, Schrödinger LLC) (Delano 2005). Subsequently, the complexes were saved in the PDB format and uploaded to the Protein-Ligand Interaction Profiler (PLIP) (https://projects.biotec.tudresden.de/plip-web/plip) (Salentin et al. 2015) and Proteins Plus (https://proteins.plus) web servers (Stierand et al. 2006; Fricker et al. 2004) for further molecular interaction analyses.

Prediction of bioactivity

Ligands bioactivity scores such as kinase inhibitors, ion channel modulators, G-Protein Couple Receptor (GPCR) ligands, enzyme inhibitors, nuclear receptor ligands, and protease inhibitors were calculated using Molinspiration online server (https://www.molinspiration.com) (Fricker et al. 2004). The scores of the organic compounds were categorized within the following range: compounds with bioactivity scores greater than zero (> 0) were classified as active. Compounds with bioactivity scores between − 5.0 and 0.0 were classified as "moderately active". Conversely, compounds with bioactivity scores less than − 5.0 (< -5.0), were considered "inactive" (Khan et al. 2017).

Pharmacokinetics properties prediction

The assessment of the ligands obtained from molecular docking which included the absorption, distribution, metabolism, excretion, and toxicity (ADMET) characteristics was carried out using ADMETlab (https://admetmesh.scbdd.com/service/evaluation/cal) (Dong et al. 2018) and admetSAR (http://lmmd.ecust.edu.cn/admetsar2/) (Cheng et al. 2012). The outcome of the assessment was used for the prediction of the pharmacokinetic characteristics of the ligands.

RESULTS

Drug likeness screening

The outcomes of the drug-likeness screening for the bioactive compounds retrieved from the selected four medicinal plants as well as the control drugs are presented in Table 2. The screening revealed that ten (10) out of the total twenty-three (23) bioactive compounds violated at least one of the five rules (Lipinski, Ghose, Veber, Egan, and Muegge). Consequently, ten bioactive compounds were excluded from further analysis. The remaining fourteen (13) compounds (Garcifuran B, 2-Hydroxyxanthone, 1,5-Dihydroxyxanthone, 3-Hydroxy-4-methoxyxanthone, 1,2-Dimethoxyxanthone, Rhamnetin, Napabucasin, beta-Lapachone, Lapachol, 5,7-Dihydroxydehydrioso- α -lapachone, Quercetin, Kaempferol, and Catechin) successfully adhered to the stipulated rules without any violation. However, Isoniazid violated two out of the five rules, while Ethionamide violated one rule.

Moreover, the molecular weights of the qualified compounds which ranged between 212.2 and 316.3 were found within defined Lipinski's rule of five (≤ 500Da). The XlogP and TPSA values were presented in Table 2.

Table 2
Drug-likeness screening of selected bioactive compounds and control drugs using the SwissADME online tool

S/N	Molecule	Formula	MW	XLOGP	TPSA	Lipinski #violations	Ghose #violations	Veber #violations	Egan #violations	Muegge #violations	Bioa Sco
1	Garcifuran b	C15H12O4	256.25	3.21	62.83	0	0	0	0	0	0.55
2	Cycloartenol	C30H50O	426.72	9.78	20.23	1	3	0	1	2	0.55
3	2-Hydroxyxanthone	C13H8O3	212.2	3.24	50.44	0	0	0	0	0	0.55
4	1,5-Dihydroxyxanthone	C13H8O4	228.2	2.8	70.67	0	0	0	0	0	0.55
5	3-hydroxy-4-Methoxyxanthone	C14H10O4	242.23	2.58	59.67	0	0	0	0	0	0.55
6	1,2-Dimethoxyxanthone	C15H12O4	256.25	2.91	48.67	0	0	0	0	0	0.55
7	Galactose	C6H12O6	180.16	-3.24	110.38	0	2	0	0	2	0.55
8	Tocopherols	C28H48O2	416.68	10.33	29.46	1	3	1	1	1	0.55
9	Rhamnetin	C16H12O7	316.26	1.87	120.36	0	0	0	0	0	0.55
10	Isoquercitrin	C21H20O12	464.38	0.36	210.51	2	1	1	1	3	0.17
11	Kaempferitrin	C27H30O14	578.52	-0.09	228.97	3	4	1	1	3	0.17
12	Napabucasin	C14H8O4	240.21	2.28	64.35	0	0	0	0	0	0.55
13	Beta-Lapachone	C15H14O3	242.27	2.2	43.37	0	0	0	0	0	0.85
14	Lapachol	C15H14O3	242.27	2.79	54.37	0	0	0	0	0	0.85
15	5,7-Dihydroxydehydroiso-α-lapachone	C15H12O5	272.25	2.82	83.83	0	0	0	0	0	0.56
16	1,8-cineole	C10H18O	154.25	2.74	9.23	0	1	0	0	2	0.55
17	Eugenol	C10H12O2	164.2	2.27	29.46	0	0	0	0	1	0.55
18	Quercetin	C15H10O7	302.24	1.54	131.36	0	0	0	0	0	0.55
19	Kaempferol	C15H10O6	286.24	1.9	111.13	0	0	0	0	0	0.55
20	Catechin	C15H14O6	290.27	0.36	110.38	0	0	0	0	0	0.55
21	Nepetrin	C22H22O12	478.4	1.43	199.51	2	0	1	1	3	0.17
22	Rutin	C27H30O16	610.52	-0.33	269.43	3	4	1	1	4	0.17
23	Terpinen-4-ol	C10H18O	154.25	3.26	20.23	0	1	0	0	2	0.55
24	Isoniazid (INH)	C6H7N3O	137.14	-0.7	68.01	0	3	0	0	1	0.55
25	Ethionamide	C8H10N2S	166.24	1.07	71	0	0	0	0	1	0.55

Molecular docking and the interaction of Mycobacterium tuberculosis enoyl-acyl carrier protein (ACP)-reductase (InhA) and ligands

The interactions between the fifteen ligands (thirteen bioactive compounds and two control drugs) and *Mycobacterium tuberculosis* enoyl-acyl carrier protein (ACP)-reductase (InhA) are presented in Table 3. These included electrostatic energy, binding efficiency, hydrophobic interactions, and hydrogen bonding interactions. The results provide insight into the binding affinity of the bioactive compounds with the target protein (InhA).

Garcifuran B, 2-Hydroxyxanthone, 1,5-Dihydroxyxanthone, 3-hydroxy-4-methoxyxanthone, and 1,2-dimethoxyxanthone present in *Garcinia kola* exhibited binding energies of -8.5, -8.8, -8.1, -8.9, and − 8.5 kcal/mol, respectively. Among the compounds, 3-hydroxy-4-methoxyxanthone had the highest binding affinity among compounds selected from *G. kola*. The interactions between these compounds and InhA are visually represented in Fig. 3. Garcifuran B established three hydrogen bonds with Gly14, Ile15, and Phe41 and had hydrophobic interactions with Phe41, Val65, Ile95, and Ile122 (Fig. 3a). Notably, a pi-stacking bond was also established with Phe41. Similarly, 2-Hydroxyxanthone engaged in two hydrogen bonds with Gly14 and Thr39. It also interacted hydrophobically with Phe41, Val65, Ile95, Phe97, and Ile122; with a pi-stacking interaction with Phe41 (Fig. 3b). The interactions of 1,5-Dihydroxyxanthone (Fig. 3c), 3-hydroxy-4-methoxyxanthone (Fig. 3d), and 1,2-dimethoxyxanthone (Fig. 3e) with InhA are similarly outlined.

Rhamnetin was identified as the only drug-like compound among the bioactive compounds selected in *M. oleifera*. It exhibited binding energy of -8.3 kcal/mol (Table 3). Rhamnetin established two hydrogen bonds with Gly14 and Thr39 and showed hydrophobic interactions with Ile16, Phe41, and Ile95 (Fig. 4).

Napabucasin, beta-Lapachone, Lapachol, and 5,7-Dihydroxydehydroiso-α-lapachone have been found to be bioactive compounds with drug-like properties in *N. laevis*. They exhibited binding energies of -9.1, -9.5, -8.5, and − 9.2 kcal/mol, respectively (Table 3). Among the compounds, Beta-Lapachone had the

highest binding affinity. Figure 5 illustrates the interactions of the ligands with the InhA protein. Napabucasin established a hydrogen bond with Gly14, engaged in hydrophobic interactions with Phe41, Leu63, Ile95, Phe97, and Ile122, and formed a π stacking interaction with Phe41 (Fig. 5a). Beta-Lapachone formed two hydrogen bonds with Gly14 and Phe41. It also exhibited hydrophobic interactions with Phe41, Val65, and Ile122, and formed a π stacking interaction with Phe41 (Fig. 5b). Similarly, Lapachol established two hydrogen bonds with Gly14 and Phe41. It demonstrated hydrophobic interactions with Phe41, Val65, and Ile122, and formed a π stacking interaction with Phe41 (Fig. 5c). In addition, 5,7-Dihydroxydehydroiso-α-lapachone interacted with Gly14 and Val65 through hydrogen bonds. It also engaged in hydrophobic interactions with Phe41, Val65, Ile95, Phe97, and Ile122 and formed a π stacking interaction with Phe41 (Fig. 5d).

In *O. gratissimum*, Quercetin, Kaempferol, and Catechin were identified to have drug-likeness properties with binding energies of -8.2, -8.1, and – 8.0 kcal/mol, respectively. Among these, Quercetin exhibited the highest binding affinity (Table 3). Quercetin established two hydrogen bonds with Gly14 and Thr39 and interacted hydrophobically with Ile16, Phe41, and Ile95 (Fig. 6). Kaempferol formed three hydrogen bonds with Gly14, Ile15, and Phe41. It also engaged in hydrophobic interactions with Ile16, Phe41, and Val65, and formed a π stacking interaction with Phe41 (Fig. 6b). Catechin interacted with Leu63 and Ser94 through hydrogen bonds, exhibited hydrophobic interactions with Ile16, Val65, Ile95, and Ile122, and formed a π stacking interaction with Phe41 (Fig. 6c).

In this study, bioactive compounds that satisfied the drug-likeness screening showed higher binding affinities to the target protein than the control drugs (Table 3). Figure 7 provides visual representations of the control drugs' interactions with InhA, indicating their penetration into the substrate metabolism site within the target protein.

Table 3
Molecular interactions of the bioactive compounds and the control drugs with the target protein (InhA) active sites

S/N	Plant source	Molecule	Binding energy (kcal/mol)	No of hydrogen bonds formed	Residues involved in hydrogen bond formation (Å)	Residue involved in hydrophobic interaction(Å)	Residue involved in π-stacking (Å)	Halogen bonds
1	*Garcinia kola*	Garcifuran B	-8.5	3	GLY14(2.18) ILE15(3.11) PHE41(2.71)	PHE41(3.25) VAL65(3.98) ILE95(3.73) ILE122(3.38)	PHE41(3.65)	
2		2-Hydroxyxanthone	-8.8	2	GLY14(1.89) THR39(2.53)	PHE41(3.47) VAL65(3.54) ILE95(3.64) PHE97(3.99, 3.67) ILE122(3.49, 3.77)	PHE41(4.02, 4.07)	
3		1,5-Dihydroxyxanthone	-8.1	1	VAL65(2.05)	PHE41(3.50) ILE95(3.84) PHE97(3.41) ILE122(3.64)	PHE41(3.98)	
4		3-hydroxy-4-methoxyxanthone	-8.9	4	GLY14(1.86) ILE15(3.33) PHE41(3.24) VAL65(3.07)	PHE41(3.59, 3.99, 3.69) PHE97(3.80, 3.50) ILE122(3.96, 3.62)	PHE41(3.97)	
5		1,2-dimethoxyxanthone	-8.5	1	GLY14(2.04)	PHE41(3.65, 3.98, 3.41) VAL65(3.72) ILE95(3.57) PHE97(3.34) ILE122(3.26)	PHE41(3.76)	
6	*Moringa oleifera*	Rhamnetin	-8.3	2	GLY14(2.14) THR39(3.23)	ILE16(3.88, 3.70, 3.70) PHE41(3.70, 3.80) ILE95(3.96, 3.66)	-	-
7	*Newbouldia laevis*	Napabucasin	-9.1	1	GLY14(2.03)	PHE41(3.87, 3.52) LEU63(3.26) ILE95(3.45, 3.95) PHE97(3.41) ILE122(3.59)	PHE41(3.87)	-
8		Beta-Lapachone	-9.5	2	GLY14(2.23) PHE41(3.42)	PHE41(3.82) VAL65(3.49) ILE122(3.42)	PHE41(3.65)	-
9		Lapachol	-8.5	2	GLY14(2.61) PHE41(3.12)	PHE41(3.82) VAL65(3.49) ILE122(3.42)	PHE41(4.03)	-

S/N	Plant source	Molecule	Binding energy (kcal/mol)	No of hydrogen bonds formed	Residues involved in hydrogen bond formation (Å)	Residue involved in hydrophobic interaction(Å)	Residue involved in π-stacking (Å)	Halogen bonds
10		5,7-Dihydroxydehydroiso-α-lapachone	-9.2	4	GLY14(3.31) VAL65(2.92)	PHE41(3.58, 3.81, 3.64) VAL65(3.60) ILE95(3.76, 3.98) PHE97(3.44) ILE122(3.60)	PHE41(3.76)	-
11	*Ocimum gratissimum*	Quercetin	-8.2	2	GLY14(2.15) THR39(2.60)	ILE16(3.92, 3.72, 3.73) PHE41(3.78, 3.80) ILE95(3.91, 3.67)	-	-
12		Kaempferol	-8.1	3	GLY14(2.69) ILE15(3.06) PHE41(3.37)	ILE16(3.84, 3.61) PHE41(3.54) VAL65(3.79)	PHE14(3.85)	-
13		Catechin	-8.0	2	LEU63(2.12) SER94(1.96)	ILE16(3.65) VAL65(3.77) ILE95(3.52, 3.73) ILE122(3.92)	PHE41(4.44)	-
14	Control Drugs	Isoniazid (Inh)	-6.1	4	GLY14(3.09) THR39(2.66) PHE41(3.37) LEU63(2.09)	PHE41(3.62) VAL65(3.84)	PHE41(3.93)	-
15		Ethionamide	-6.0	2	GLY14(3.17) PHE41(3.24)	PHE41(3.65, 3.93, 3.69) VAL65(3.87) PHE97(3.75) ILE122(3.64)	PHE41(3.80)	-

Predicted bioactivity

The predicted bioactivity scores of the bioactive compounds and the control drugs, assessed from ion channel modulator, GPCR ligand, nuclear receptor ligand, protease inhibitor, kinase inhibitor, and enzyme inhibitor are presented in Table 4.

Notably, all compounds including Isoniazid and Ethionamide fall within the bioactivity score range of -5.0 to 0.0 for the GPCR ligand category, showing a moderate level of activity. An exception is Catechin, which possesses a bioactivity score greater than 0.0, hence, signifying its active status. For the ion channel modulator category, the bioactivity scores range from − 5.0 to 0.0 for 2-Hydroxyxanthone, 1,5-Dihydroxyxanthone, 3-Hydroxy-4-methoxyxanthone, 1,2-Dimethoxyxanthone, Rhamnetin, Napabucasin, 5,7-Dihydroxydehydroiso-α-Lapachone, Quercetin, Kaempferol, Isoniazid (INH), and Ethionamide, showing moderate activity. However, Garcifuran B, beta-Lapachone, Lapachol, and Catechin exhibit bioactivity scores greater than 0.0, indicating high activity.

Similarly, in the context of kinase inhibitor activity, 2-Hydroxyxanthone, 3-Hydroxy-4-methoxyxanthone, 1,2-Dimethoxyxanthone, Napabucasin, beta-Lapachone, Lapachol, 5,7-Dihydroxydehydroiso-α-Lapachone, Isoniazid (INH), and Ethionamide showcase bioactivity scores ranging from − 5.0 to 0.0, denoting moderate activity. In contrast, Garcifuran B, 1,5-Dihydroxyxanthone, Rhamnetin, Quercetin, Kaempferol, and Catechin exhibit bioactivity scores greater than 0.0, indicating their high activity in the context of kinase inhibition.

Garcifuran B, 2-Hydroxyxanthone, 3-Hydroxy-4-methoxyxanthone, 1,2-Dimethoxyxanthone, Napabucasin, Isoniazid (INH), and Ethionamide exhibited moderate bioactivity scores as nuclear receptor ligands ranging from − 5.0 to 0.0. In contrast, 1,5-Dihydroxyxanthone, Rhamnetin, beta-Lapachone, Lapachol, 5,7-Dihydroxydehydroiso-α-Lapachone, Quercetin, Kaempferol, and Catechin were considered active with nuclear receptor-ligand interaction with bioactivity scores greater than 0.0. Moreover, the bioactivity scores of all compounds excluding beta-Lapachol and Catechin, ranged from − 5.0 to 0.0, indicating moderate activity as protease inhibitors. Also, within the enzyme inhibitor category, all compounds, except Napabucasin, Isoniazid (INH), and Ethionamide exhibited bioactivity scores greater than 0.0, suggesting their high activity as enzyme inhibitors.

Table 4
Predicted bioactivity scores for selected bioactive compounds and control drugs

S/N	Bioactive Compound	GPCR ligand	Ion channel modulator	Kinase inhibitor	Nuclear receptor ligand	Protease inhibitor	Enzyme inhibitor
1	Garcifuran B	-0.07	0.06	0.09	-0.06	-0.41	0.11
2	2-Hydroxyxanthone	-0.40	-0.21	-0.32	-0.15	-0.67	0.07
3	1,5-Dihydroxyxanthone	-0.40	-0.18	0.25	0.08	-0.46	0.27
4	3-Hydroxy-4-methoxy Xanthone	-0.47	-0.18	-0.38	-0.28	-0.69	0.07
5	1,2-Dimethoxyxanthone	-0.30	-0.24	-0.17	-0.09	-0.49	0.07
6	Rhamnetin	-0.11	-0.27	0.21	0.27	-0.27	0.20
7	Napabucasin	-0.58	-0.47	-0.35	-0.45	-0.61	-0.05
8	beta-Lapachone	-0.08	0.33	-0.25	0.07	0.08	0.45
9	Lapachol	-0.17	0.27	-0.11	0.20	-0.09	0.65
10	5,7-Dihydroxy dehydroiso- α - Lapachone	-0.18	-0.34	-0.32	0.30	-0.38	0.42
11	Quercetin	-0.06	-0.19	0.28	0.36	-0.25	0.28
12	Kaempferol	-0.10	-0.21	0.21	0.32	-0.27	0.26
13	Catechin	0.41	0.14	0.09	0.60	0.26	0.47
14	Isoniazid (Inh)	-1.39	-1.45	-1.05	-2.33	-1.23	-0.66
15	Ethionamide	-0.97	-1.11	-1.63	-1.55	-1.68	-0.53

Pharmacokinetics properties prediction

Drug development involves the assessment of the absorption, distribution, metabolism, excretion, and toxicity (ADMET) properties of bioactive compounds. As reported by Umar et al. (2021) for a small ligand to be potent, it should not only reach its target in the body at a substantial concentration but also maintain its bioactive characteristics for a long period. Tables 5 and 6 provide the ADMET properties for the bioactive compounds and the control drugs, respectively. However, the 2D molecular structures of these compounds are depicted in Figs. 8 and 9.

In terms of drug absorption, beta-Lapachone, Lapachol, Isoniazid, and Ethionamide were predicted to be capable of penetrating the blood-brain barrier (BBB) (Table 5). Among the hit ligands, Gacifuran B, 1,2-Dimethoxyxanthone, Napabucasin, beta-Lapachone, Lapachol, 5,7-Dihydroxydehydroiso-alpha-lapachone, and the control drugs demonstrated low absorption in the intestine through Caco-2 permeability assessment. Regarding drug distribution, most compounds were expected to accumulate in the mitochondria. However, Ethionamide was projected to be localized in lysosomes.

2-Hydroxyxanthone, 3-hydroxy-4-methoxyxanthone, 1,2-dimethoxyxanthone, quercetin, catechin, isoniazid, and ethionamide did not exhibit enzyme inhibition against CYP450 2C9. Similarly, 1,5-Dihydroxyxanthone, Napabucasin, Lapachone, Quercetin, Catechin, and the control drugs did not indicate inhibition of CYP450 2C19. Conversely, 3-hydroxy-4-methoxyxanthone, 1,2-dimethoxyxanthone, Rhamnetin, beta-Lapachone, 5,7-Dihydroxydehydroiso-alpha-lapachone, Quercetin, and Kaempferol were predicted to be substrates of CYP450 3A4. Furthermore, 1,2-dimethoxyxanthone, beta-Lapachone, Quercetin, and Kaempferol were also indicated as potential inhibitors of CYP450 3A4. In terms of toxicity, all compounds, including the control drugs, except Gacifuran B, Rhamnetin, and Catechin, were projected to potentially induce hepatotoxicity in humans. However, the compounds and control drugs showed no carcinogenicity potential. This comprehensive ADMET analysis provides crucial insights into the potential behavior of these compounds within biological systems and their potential therapeutic application.

Table 6
Predicted ADMET properties of control drugs

S/N	PROPERTIES	Isoniazid	Ethionamide
1 Absorption	Caco-2 permeability	Yes	Yes
	Pgp-inhibitor	No	No
	Pgp-Substrate	No	No
2 Distribution	BBB	Yes	Yes
	PPB	8.9995%	28.86%
	Sub-cellular localization	Mitochondria	Lysosomes
3 Metabolism	CYP 1A2 inhibition	Yes	Yes
	CYP 3A4 inhibition	No	No
	CYP 3A4 substrate	No	No
	CPY 2C9 inhibition	No	No
	CYP 2C9 substrate	No	No
	CYP2C19 inhibition	No	No
	CYP 2D6 inhibition	No	No
	CYP 2D6 substrate	No	No
	Uct catalyzed	No	No
4 Toxicity	Acute oral toxicity	Class iii	Class iii
	hERG inhibitor	No	No
	Human hepatotoxicity	Yes	Yes
	Ames mutagenicity	Yes	No
	Carcinogenicity	No	No

BBB means blood-brain barrier; PPB - plasma protein binding; hERG - human ether-a-go-go.

DISCUSSION

The increasing rate of tuberculosis bacteria resistance to drugs (streptomycin, ethambutol, isoniazid, rifampicin, and pyrazinamide) used for its treatment has necessitated the need for novel medications for its management and cure.

In this study, thirteen bioactive compounds (Garcifuran B, 2-Hydroxyxanthone, 1,5-Dihydroxyxanthone, 3-Hydroxy-4-methoxyxanthone, 1,2-Dimethoxyxanthone, Rhamnetin, Napabucasin, beta-Lapachone, Lapachol, 5,7-Dihydroxydehydroiso-alpha-lapachone, Quercetin, Kaempferol, Catechin) showed zero violation to drug-likeness rules while also presenting molecular weights within the Lipinski-defined range (< 500 daltons). The success of the drug-likeness screening of these bioactive compounds informed their likelihood of becoming an orally administrable drug (Ullah et al. 2020). For instance, Lipinski's rule of five evaluates a compound's potential for oral availability based on parameters like molecular weight and partition coefficient (Daina et al. 2017). Compounds with a molecular weight of 500 Daltons or lower are deemed suitable for oral drug development. Moreover, the values of Molecular Lipophilicity Potential (XlogP) and Topological Polar Surface Area (TPSA) play pivotal roles in determining a drug's permeability and ultimately its oral bioavailability. XlogP measures a compound's distribution coefficient between n-octanol and water, influencing its interactions with cellular membranes and other proteins (Gou et al. 2021). Notably, all thirteen bioactive compounds and the control drugs in this study exhibited XlogP values below five, implying an affinity for hydrophilic environments (Piccirillo and Amaral, 2018). Collectively, these analyses underscore the favorable drug-likeness attributes of the bioactive compounds studied, suggesting their potential suitability as orally administered drugs. The adherence to Lipinski's rule of five, the appropriate XlogP values, and the molecular characteristics that facilitate cellular interactions contribute to the compounds' overall potential as effective and viable candidates for drug development.

The binding interaction between ligand and protein offers insights into their shape and electrostatic relationships. Moreover, it predicts the binding conformation and orientation of the ligand within the protein's binding pocket, and how the ligand binds to residues in the enzyme's active site. The docking score represents the total energy of the interaction, with lower negative values depicting stronger interactions (Kannan et al. 2016). This study highlighted

Beta-Lapachone derived from *N. laevis* as the compound with the highest binding affinity compared to other compounds and the standard drugs (Table 3). Beta-Lapachone exhibited a strong binding energy of -9.5 kcal/mol. Following closely are, 5,7-Dihydroxydehydroiso-alpha-lapachone and Napabucasin from *N. laevis* that exhibited the binding energy of -9.2 kcal/mol and − 9.1 kcal/mol, respectively. Subsequently, 3-Hydroxy-4-methoxyxanthone and 2-Hydroxyxanthone from *G. kola* showed the binding energy of -8.9 kcal/mol and − 8.8 kcal/mol, respectively. Garcifuran B, 1,2-Dimethoxyxanthone, and Lapachol, derived from *G. kola* and *N. laevis*, all shared a binding energy of -8.5 kcal/mol. Rhamnetin from *M. oleifera* had a binding energy of -8.3 kcal/mol, followed by Quercetin in *O. gratissimum* with − 8.2 kcal/mol. 1,5-Dihydroxyxanthone in *G. kola* and Kaempferol in *O. gratissimum* both had binding energies of -8.1 kcal/mol. The compound with the lowest binding affinity was Catechin from *G. kola*, exhibiting a binding energy of -8.0 kcal/mol. Notably, all the bioactive compounds that passed the drug-likeness examination had higher binding affinities with the protein than the control drugs. This suggests their potential to hinder the activities of *Mycobacterium tuberculosis*, offering a potential avenue for combating its effects. The binding of these compounds to InhA was also predicted to hinder the entry of incoming substrates. This interaction has the potential to limit bacterial infection and granuloma formation, which are characteristics of tuberculosis. By interacting with this protein, these compounds could help mitigate the adverse effects associated with these processes caused by *Mycobacterium tuberculosis*.

Binding the bioactive compounds to the *Mycobacterium tuberculosis* enoyl-acyl carrier protein (ACP)-reductase (InhA) target offers promising anti-tubercular potential by inhibiting the target's activity. The compounds' capability to bind to the catalytic sites of this target was observed, suggesting their potential as inhibitors. In comparison to the control drugs, the studied compounds displayed better binding affinities to InhA, indicating their potency as inhibitors and potential anti-tuberculosis agents. The ligand Beta-Lapachone, which exhibited the highest docking score, showed strong binding affinity to specific amino acid residues. Beta-Lapachone had hydrogen interactions with Gly14 and Phe41, while hydrophobic interactions were established with Phe41, Val65, and Ile122. Similarly, 5,7-Dihydroxydehydroiso-alpha-lapachone showed hydrogen interaction with Gly14 and Val65, along with hydrophobic interactions involving Phe41, Val65, Ile95, Phe97, and Ile122. Napabucasin's interactions included hydrogen bonds with Gly14 and hydrophobic interactions with Phe41, Leu63, Ile95, Phe97, and Ile122. 3-Hydroxy-4-methoxyxanthone formed hydrogen bonds with Gly14, Ile15, Phe41, and Val65, and hydrophobic interactions with Phe41, Phe97, and Ile122. 2-Hydroxyxanthone exhibited hydrogen interactions with Gly14 and Thr39, and hydrophobic interactions with Phe41, Val65, Ile95, Fhe97, and Ile122. Garcifuran B's interactions included hydrogen bonds with Gly14, Ile15, and Phe41, and hydrophobic interactions with Phe41, Val65, Ile95, and Ile122. Similar interactions were observed for other compounds like 1,2-Dimethoxyxanthone, Lapachol, Rhamnetin, Quercetin, 1,5-Dihydroxyxanthone, Kaempferol, and Catechin, with variations in the specific amino acid residues involved in the interactions. All compounds, except Rhamnetin and Quercetin, exhibited parallel pi-stacking interactions with Phe41. These residues collectively formed a binding pocket for the ligands. A study by Chollet et al. (2018) identified interacting residues of InhA, many of which overlapped with the findings of the current study. The interaction of the ligands with these residues suggests their potential to minimize resistance to tuberculosis. In summary, the inhibition of InhA by Beta-Lapachone, 5,7-Dihydroxydehydroiso-alpha-lapachone, Napabucasin, 3-Hydroxy-4-methoxyxanthone, 2-Hydroxyxanthone, Garcifuran B, 1,2-Dimethoxyxanthone, Lapachol, Rhamnetin, Quercetin, 1,5-Dihydroxyxanthone, Kaempferol, and Catechin derivatives relies on their ability to form diverse bonds with the active sites of amino acid residues. Additionally, the compounds' ability to selectively interact with these active site residues is instrumental in reducing the likelihood of adverse or toxic effects. Interactions involving lipophilicity, hydrogen bonding, and pi-stacking are pivotal in the interactions between the compounds and proteins at the active site, contributing to the compounds' potential as anti-tuberculosis agents.

The ability of a drug to bind to biological targets such as ion channels, receptors, and enzymes showcases its pharmacological activities (Khan et al. 2017). This study shows that the top compounds, along with the control drugs Isoniazid and Ethionamide had bioactivity scores greater than − 5.0 (< -5.0). This suggests that they are all active in binding to GPCR and nuclear receptor ligands, modulating ion channels, inhibiting kinases, proteases, and enzyme activity.

ADMET properties of compounds play important roles in drug development. The rate and extent of absorption of drugs from its administration site (e.g. oral, intravenous, topical) to the bloodstream influence how quickly and efficiently a drug reaches its target site. Moreover, the extent of distribution of drugs to the body tissues and organs is influenced by factors such as blood flow, tissue permeability, and the drug’s affinity for various tissues. Metabolism, primarily occurring in the liver can alter a drug's chemical structure, and affect its activity and duration of action. Whereas, excretion involves the elimination of a drug and its metabolites from the body through the kidneys via urine; however, drugs can also be excreted through bile, sweat, and other routes. These properties are crucial in determining a compound's pharmacological characteristics and its ability to effectively reach and remain at the target protein to exert its therapeutic effects (Balogun et al. 2020). The pharmacokinetic profile stated in Table 5 revealed that none of the compounds, including the two control drugs, were substrates of P-glycoprotein. Lin and Yamazaki (2003) reported that P-glycoprotein is an ATP-binding cassette (ABC) protein responsible for transporting molecules out of cells, preventing their bioaccumulation, and eliciting their response; hence, qualifying the compounds as potential drugs. However, there is a need for pharmacophoric modeling, which can improve some of the fundamental ADMET properties of the ligands.

Plasma protein binding (PPB) plays a critical role in drug uptake and distribution within the body. It also significantly impacts a drug's pharmacodynamic behavior. The process of drug binding to plasma proteins can affect its oral bioavailability, as it determines the concentration of the drug that remains free and active in the bloodstream. Drugs with high protein binding may exhibit a low therapeutic index, as they have limited free drugs available for activity. Notably, 1,2-Dimethoxyxanthone has a PPB value of less than 90%, suggesting a potentially high therapeutic index. Cytochrome P450 (CYP) enzymes are essential in drug metabolism, particularly in the phase 1 metabolism of various xenobiotics. Esteves et al. (2012) reported that compounds capable of inhibiting specific CYP isoforms can lead to drug-drug interactions. In the context of this study, it was predicted that 2-Hydroxyxanthone, 3-hydroxy-4-methoxyxanthone, 1,2-dimethoxyxanthone, Quercetin, Catechin, Isoniazid, and Ethionamide would not inhibit the CYP2C9 isoform. Similarly, 1,5-Dihydroxyxanthone, Napabucasin, Lapachone, Quercetin, Catechin, and the control drugs were also predicted not to inhibit the CYP450 2C19 isoform. In addition, all compounds except Beta-Lapachone were expected to be non-inhibitors of the CYP450 2D6 isoform, suggesting that they are unlikely to induce drug-drug interactions that could result in loss of efficacy.

Carcinogenicity is a critical concern when evaluating the toxicity profile of drugs, as carcinogenic substances can potentially harm the human physiological system by interfering with cellular metabolic processes (Gou et al. 2021). All the hit ligands including the control drugs were predicted to be non-

carcinogenic. This could be ascribed to their ability to pass the inflexible drug-likeness screening. The non-carcinogenic properties of the hit ligands suggest their suitability as potential drugs.

The present study indicates that the selected active compounds in the studied medicinal plants, especially Beta-Lapachone, 5,7-Dihydroxydehydroiso-a-lapachone, Napabucasin, 3-Hydroxy 4-methoxyxanthone, 2-Hydroxyxanthone, Garcifuran B, 1,2-Dimethoxyxanthone, Lapachol, Rhamnetin, Quercetin, 1,5-Dihydroxyxanthone, Kaempferol, and Catechin, possess a strong in silico inhibitory effect against InhA through molecular docking techniques. These findings are valuable for selecting promising compounds, designing effective drug formulations, and ensuring patient safety. However, the outcomes should be validated through molecular dynamic simulations and other laboratory studies.

CONCLUSIONS

The study identified thirteen (13) bioactive compounds from four medicinal plants (*Garcinia kola*, *Moringa oleifera*, *Newbouldia laevis*, and *Ocimum gratissimum*) that successfully passed the drug-likeness screening. These compounds Beta-Lapachone, Napabucasin, 2-Hydroxyxanthone, 3-Hydroxy 4-methoxyxanthone, 1,2-Dimethoxyxanthone, 5,7-Dihydroxydehydroiso-alpha-lapachone, Lapachol, 1,5-Dihydroxyxanthone, Rhamnetin, Kaempferol, Quercetin, Catechin, and Garcifuran B exhibited the potential to function as tuberculosis drugs. Furthermore, the molecular docking analysis of the ligands with InhA demonstrated all the bioactive compounds exhibited higher binding affinity compared to the control drugs. This suggests them as hit ligands with potential antitubercular activities. This study established that compounds sourced from *G. kola*, *M. oleifera*, *N. laevis*, and *O. gratissimum* exhibited favorable docking interactions with the target protein (InhA) compared with the control drugs (Isoniazid and Ethionamide). Therefore, could be considered as potential compounds to be used in the treatment of tuberculosis. However, we recommend further experimental assessments of the lead compounds to confirm the computational results. Future research should also include a wider variety of bioactive compounds and molecular dynamics simulations to explore protein-ligand complex stability and molecular interactions.

Declarations

Conflict of interest statement

The authors declare that there is no conflict of interest associated with the publication of the manuscript.

Author Contribution

Conceptualization; O.O.F and A.A.MMethodology: B.R.L and A.A.MWriting- original draft preparation: B.R.L. and O.O.F.Writing- Review and Editing: A.O.B. and S.A.PSupervision: O.O.F.

References

1. Anaduaka EG, Ogugua VN, Egba SI, Apeh VO (2013) Investigation of some important phytochemical, nutritional properties and toxicological potentials of ethanol extracts of Newbouldia laevis leaf and stem. Afr J Biotechnol, 12(40)
2. Atanasov AG, Waltenberger B, Pferschy-Wenzig EM, Linder T, Wawrosch C, Uhrin P, Temml V, Schwaiger S, Heiss WH, Rollinger JM, Schuster D, Breuss JM, Bochkov V, Mihovilovic MD, Kopp B, Bauer R, Dirsch VM, Stuppner H (2015) Discovery and resupply of pharmacologically active plant-derived natural products: A review. Biotechnol Adv 33(8):1582–1614
3. Balogun TA, Omoboyewa DA, Saibu OA (2020) In silico anti-malaria activity of quinolone compounds against Plasmodium falciparum dihydrofolate reductase (pfDHFR). Int J Biochem Res Rev 29(8):10–17
4. Berman HM, Bhat TN, Bourne PE, Feng Z, Gilliland G, Weissig H, Westbrook J (2000) The Protein Data Bank and the challenge of structural genomics. Nat Struct Biol 7(11):957–959
5. Bhattacharya A, Tiwari P, Sahu PK, Kumar S (2018) A review of the phytochemical and pharmacological characteristics of Moringa oleifera. J Pharm bioallied Sci 10(4):181
6. Bickerton GR, Paolini GV, Besnard J, Muresan S, Hopkins AL (2012) Quantifying the chemical beauty of drugs. Nat Chem 4(2):90–98
7. Buba CI, Okhale SE, Muazzam I (2016) Garcinia kola: The phytochemistry, pharmacology and therapeutic applications. Int J Pharmacognosy 3(2):67–81
8. Cheng F, Li W, Zhou Y, Shen J, Wu Z, Liu G, Lee PW, Tang Y (2012) admetSAR: a comprehensive source and free tool for assessment of chemical ADMET properties. J Chem Inf Model 52(11):3099–3105
9. Chollet A, Maveyraud L, Lherbet C, Bernardes-Génisson V (2018) An overview on crystal structures of InhA protein: Apo-form, in complex with its natural ligands and inhibitors. Eur J Med Chem 146:318–343
10. Daina A, Michielin O, Zoete V (2017) SwissADME: a free web tool to evaluate pharmacokinetics, drug-likeness and medicinal chemistry friendliness of small molecules. Sci Rep 7(1):42717
11. Delano The PyMOL molecular graphics system, DeLano Scientific LLC, 400 Oyster Point Blvd., Suite 213, South San Francisco, 2005. CA 94080 – 1918
12. Dermane A, Kpegba K, Eloh K, Osei-Safo D, Amewu RK, Caboni P (2020) Differential constituents in roots, stems and leaves of Newbouldia laevis Thunb. screened by LC/ESI-Q-TOF-MS. Results in Chemistry 2:100052

13. Dong J, Wang NN, Yao ZJ, Zhang L, Cheng Y, Ouyang D, Lu AP, Cao DS (2018) ADMETlab: a platform for systematic ADMET evaluation based on a comprehensively collected ADMET database. J Cheminform 10:1–11
14. Edo GI, Samuel PO, Ossai S, Nwachukwu SC, Okolie MC, Oghenegueke O, Asaah EU, Akpoghelie PO, Ugbune U, Owheruo JO, Ezekiel GO (2023) Phytochemistry and pharmacological compounds present in scent leaf: A review. Food Chemistry Advances, 3, p.100300
15. Egan WJ, Merz KM, Baldwin JJ (2000) Prediction of drug absorption using multivariate statistics. J Med Chem 43(21):3867–3877
16. Emmanuel O, Uche ME, Dike ED, Etumnu LR, Ugbogu OC, Ugbogu EA (2022) A review on *Garcinia kola* heckel: traditional uses, phytochemistry, pharmacological activities, and toxicology. Biomarkers 27(2):101–117
17. Emmanuel O, Uche ME, Dike ED, Etumnu LR, Ugbogu OC, Ugbogu EA (2022) A review on Garcinia kola Heckel: Traditional uses, phytochemistry, pharmacological activities, and toxicology. Biomarkers 27(2):101–117
18. Espinal MA (2003) The global situation of MDR-TB. Tuberculosis 83(1–3):44–51
19. Esteves F, Rueff J, Kranendonk M (2021) The central role of cytochrome P450 in xenobiotic metabolism- a brief review on a fascinating enzyme family. J xenobiotics 11(3):94–114
20. Farjallah A, Chiarelli LR, Forbak M, Degiacomi G, Danel M, Goncalves F, … and, Chassaing S (2021) A coumarin-based analogue of thiacetazone as dual covalent inhibitor and potential fluorescent label of HadA in Mycobacterium tuberculosis. ACS Infect Dis 7(3):552–565
21. Fricker PC, Gastreich M, Rarey M (2004) Automated drawing of structural molecular formulas under constraints. J Chem Inf Comput Sci 44(3):1065–1078
22. Gormann R, Kaloga M, Li XC, Ferreira D, Bergenthal D, Kolodziej H (2003) Furanonaphthoquinones, atraric acid and a benzofuran from the stem barks of Newbouldia laevis. Phytochemistry 64(2):583–587
23. Guo Y, Fan Y, Li G, Wang Z, Shi X, Shen M (2021) Cluster bomb based on redox-responsive carbon dot nanoclusters coated with cell membranes for enhanced tumor theranostics. ACS Appl Mater Interfaces 13(47):55815–55826
24. Hazbón MH, Brimacombe M, Bobadilla del Valle M, Cavatore M, Guerrero MI, Varma-Basil M, Billman-Jacobe H, Lavender C, Fyfe J, García-García L, León CI (2006) Population genetics study of Isoniazid resistance mutations and evolution of multidrug-resistant *Mycobacterium tuberculosis*. Antimicrob Agents Chemother 50(8):2640–2649
25. Hussein HA, Borrel A, Geneix C, Petitjean M, Regad L, Camproux AC (2015) PockDrug-Server: a new web server for predicting pocket druggability on holo and apo proteins. Nucleic Acids Res 43(W1):W436–W442
26. Jagadeb M, Rath SN, Sonawane A (2019) In silico discovery of potential drug molecules to improve the treatment of isoniazid-resistant Mycobacterium tuberculosis. J Biomol Struct Dyn 37(13):3388–3398
27. Jakhar R, Dangi M, Khichi A, Chhillar AK (2020) Relevance of molecular docking studies in drug designing. Curr Bioinform 15(4):270–278
28. Jayaraman M, Loganathan L, Muthusamy K, Ramadas K (2021) Virtual screening assisted discovery of novel natural products to inhibit the catalytic mechanism of Mycobacterium tuberculosis inhA. J Mol Liq 335:116204
29. Kamsri P, Hanwarinroj C, Phusi N, Pornprom T, Chayajarus K, Punkvang A, … and, Pungpo P (2019) Discovery of new and potent InhA inhibitors as antituberculosis agents: Structure-based virtual screening validated by biological assays and X-ray crystallography. J Chem Inf Model 60(1):226–234
30. Kannan R, Alharbi NS, Kadaikunnan S, Rajaram SK, Alexander RA (2016) Insilico Analysis of Phytoconstituents from Allium sativum as Potential Inhibitors of Inha in Mycobacterium tuberculosis. Brazilian Archives of Biology and Technology 59:16160109
31. Kazmi SR, Jun R, Yu MS, Jung C, Na D (2019) In silico approaches and tools for the prediction of drug metabolism and fate: A review. Comput Biol Med 106:54–64
32. Khan T, Dixit S, Ahmad R, Raza S, Azad I, Joshi S, Khan AR (2017) Molecular docking, PASS analysis, bioactivity score prediction, synthesis, characterization and biological activity evaluation of a functionalized 2-butanone thiosemicarbazone ligand and its complexes. J Chem Biol 10:91–104
33. Kuete V, Eyong KO, Folefoc GN, Beng VP, Hussain H, Krohn K, Nkengfack AE (2007) Antimicrobial activity of the methanolic extract and of the chemical constituents isolated from Newbouldia laevis. Die Pharmazie-An International Journal of Pharmaceutical Sciences 62(7):552–556
34. Lin J, Yamazaki M (2003) Role of P-glycoprotein in pharmacokinetics. Clin Pharmacokinet 42(1):59–98
35. Lipinski CA (2016) Rule of five in 2015 and beyond: Target and ligand structural limitations, ligand chemistry structure and drug discovery project decisions. Adv Drug Deliv Rev 101:34–41
36. Massengo-Tiassé RP, Cronan JE (2009) Diversity in enoyl-acyl carrier protein reductases. Cell Mol Life Sci 66:1507–1517
37. Melo RS, Azevedo A, Gomes Pereira ÁM, Rocha AM, Bastos Cavalcante RR, Matos RMC, Lopes MNR, Gomes PH, Soares Rodrigues GA, Santos TH, H.S.D. and, Ponte IL (2019) Chemical composition and antimicrobial effectiveness of Ocimum gratissimum L. essential oil against multidrug-resistant isolates of Staphylococcus aureus and Escherichia coli. Molecules, 24(21), p.3864
38. Mohr FBM, Lermen C, Gazim ZC, Gonçalves JE, Alberton O (2017) Antifungal activity, yield, and composition of Ocimum gratissimum essential oil. Genet Mol Res 16(1):1–10
39. Morrison J, Pai M, Hopewell PC (2008) Tuberculosis and latent tuberculosis infection in close contacts of people with pulmonary tuberculosis in low-income and middle-income countries: a systematic review and meta-analysis. Lancet Infect Dis 8(6):359–368
40. Muegge I, Heald SL, Brittelli D (2001) Simple selection criteria for drug-like chemical matter. J Med Chem 44(12):1841–1846
41. Natarajan A, Beena PM, Devnikar AV, Mali S (2020) A systemic review on tuberculosis. Indian J Tuberculosis 67(3):295–311
42. Padayachee B, Baijnath H (2020) An updated comprehensive review of the medicinal, phytochemical and pharmacological properties of Moringa oleifera. South Afr J Bot 129:304–316

43. Pakadang SR, Hilaria M, Dewi STR, Sinala S (2021) MIC and MKC Analysis of Herbal Medicine in Indonesia against Mycobacterium tuberculosis. Pharmacognosy J, 13(5)
44. Pettersen EF, Goddard TD, Huang CC, Couch GS, Greenblatt DM, Meng EC, Ferrin TE (2004) UCSF Chimera—a visualization system for exploratory research and analysis. J Comput Chem 25(13):1605–1612
45. Piccirillo E, Amaral ATD (2018) Virtual screening of bioactive compounds: concepts and aplications. Quim Nova 41:662–677
46. Rozwarski DA, Vilcheze C, Sugantino M, Bittman R, Sacchettini JC (1999) Crystal structure of the Mycobacterium tuberculosis enoyl-ACP reductase, InhA, in complex with NAD + and a C16 fatty acyl substrate. J Biol Chem 274(22):15582–15589
47. Salentin S, Schreiber S, Haupt VJ, Adasme MF, Schroeder M (2015) PLIP: fully automated protein–ligand interaction profiler. Nucleic Acids Res 43(W1):W443–W447
48. Samje M, Tchoufack B, Ngoufo P, Dilonga HM (2021) Evaluation of Antibacterial Activities and Cytotoxicity of Three Medicinal Plants Used for the Management of Mycobacterium Tuberculosis and Staphylococcus Aureus Infections in the North-West Region of Cameroon. J Tuberculosis Res 9(01):1
49. Stierand K, Maaß PC, Rarey M (2006) Molecular complexes at a glance: automated generation of two-dimensional complex diagrams. Bioinformatics 22(14):1710–1716
50. Tauchen J, Frankova A, Manourova A, Valterova I, Lojka B, Leuner O (2023) Garcinia kola: a critical review on chemistry and pharmacology of an important West African medicinal plant. Phytochemistry Reviews, pp 1–47
51. Trott O, Olson AJ (2010) AutoDock Vina: improving the speed and accuracy of docking with a new scoring function, efficient optimization, and multithreading. J Comput Chem 31(2):455–461
52. Ugbogu OC, Emmanuel O, Agi GO, Ibe C, Ekweogu CN, Ude VC, Uche ME, Nnanna RO, Ugbogu EA (2021) A review on the traditional uses, phytochemistry, and pharmacological activities of clove basil (*Ocimum gratissimum* L.). Heliyon, 7(11)
53. Ugboko HU, Nwinyi OC, Oranusi SU, Fatoki TH, Omonhinmin CA (2020) Antimicrobial importance of medicinal plants in Nigeria. The Scientific World Journal, 2020
54. Ullah MA, Johora FT, Sarkar B, Araf Y, Rahman MH (2020) Curcumin analogs as the inhibitors of TLR4 pathway in inflammation and their drug like potentialities: a computer-based study. J Recept Signal Transduction 40(4):324–338
55. Umar HI, Josiah SS, Saliu TP, Jimoh TO, Ajayi A, Danjuma JB (2021) In-silico analysis of the inhibition of the SARS-CoV-2 main protease by some active compounds from selected African plants. J Taibah Univ Med Sci 16(2):162–176
56. Veber DF, Johnson SR, Cheng HY, Smith BR, Ward KW, Kopple KD (2002) Molecular properties that influence the oral bioavailability of drug candidates. J Med Chem 45(12):2615–2623
57. Velayati AA, Farnia P, Masjedi MR (2013) Totally drug-resistant tuberculosis (TDR-TB): A debate on global health communities. Int J Mycobacteriology 2(2):71–72
58. World Health Organization (2023) https://www.who.int/news-room/fact-sheets/detail/tuberculosis
59. Zaku SG, Emmanuel S, Tukur AA, Kabir A (2015) Moringa oleifera: An underutilized tree in Nigeria with amazing versatility: A review. Afr J Food Sci 9(9):456–461

Tables

Table 5 is available in the Supplementary Files section.

Figures

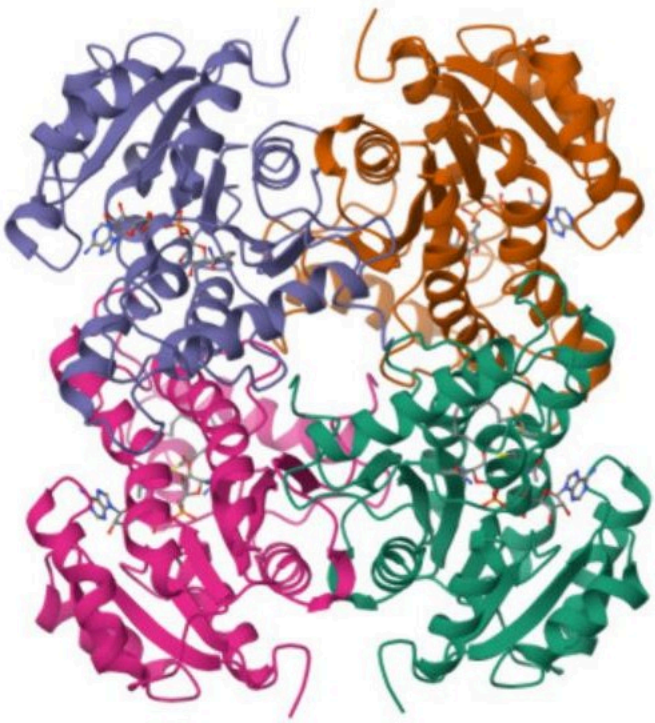

Figure 1

Structure of the *Mycobacterium tuberculosis* enoyl-acyl carrier protein (ACP)-reductase (InhA) (Adopted from protein data bank).

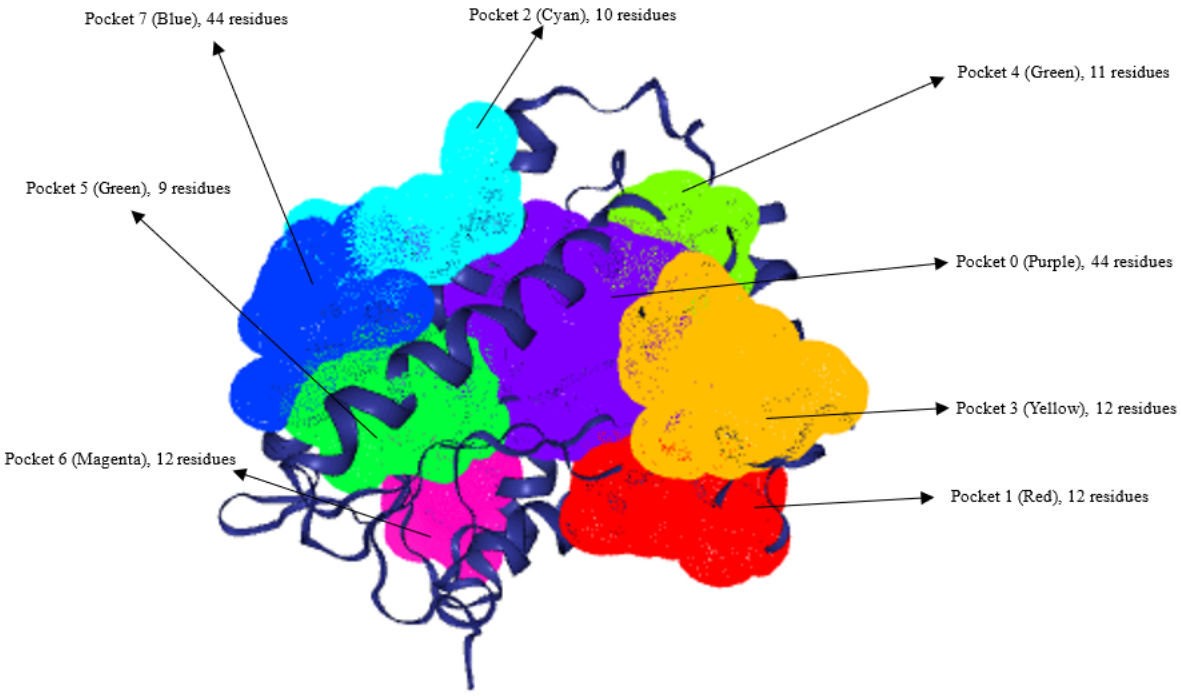

Figure 2

Structure of the *Mycobacterium tuberculosis* enoyl-acyl carrier protein (ACP)-reductase (InhA) and its binding pockets (Adopted from PockDrug web).

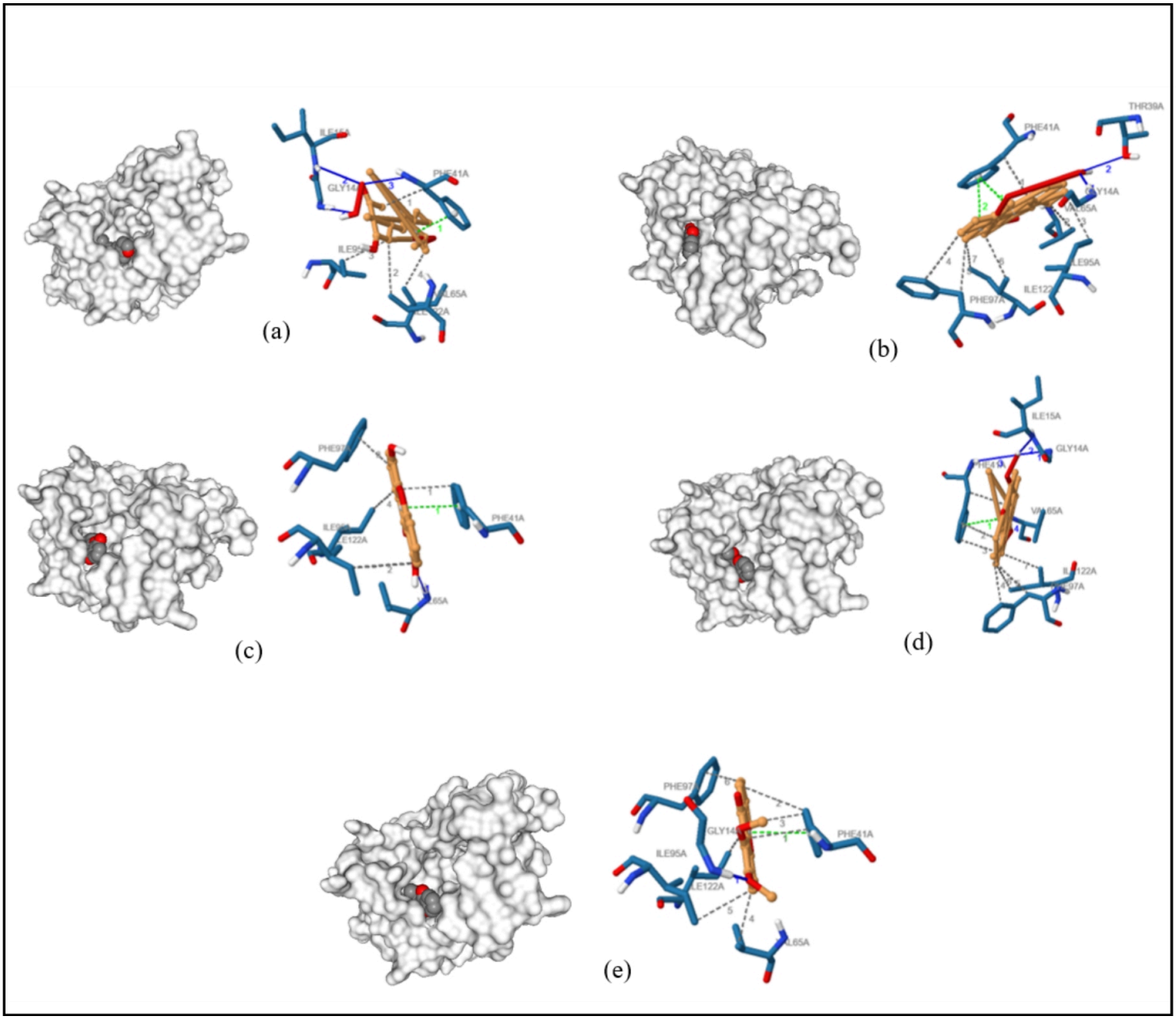

Figure 3

The binding configuration of bioactive compounds derived from *Garcinia kola*. (a) Garcifuran B, (b) 2- Hydroxyxanthone, (c) 1,5-Dihydroxyxanthone, (d) 3-hydroxy-4-methoxyxanthone and (e) 1,2- dimethoxyxanthone in the InhA active site as obtained through molecular docking utilizing AutoDock Vina. Binding interactions were presented in coloured and dotted lines. Grey dotted line –Hydrophobic interaction; Green dotted line – Pi stacking; Blue dashed line - Hydrogen bond.

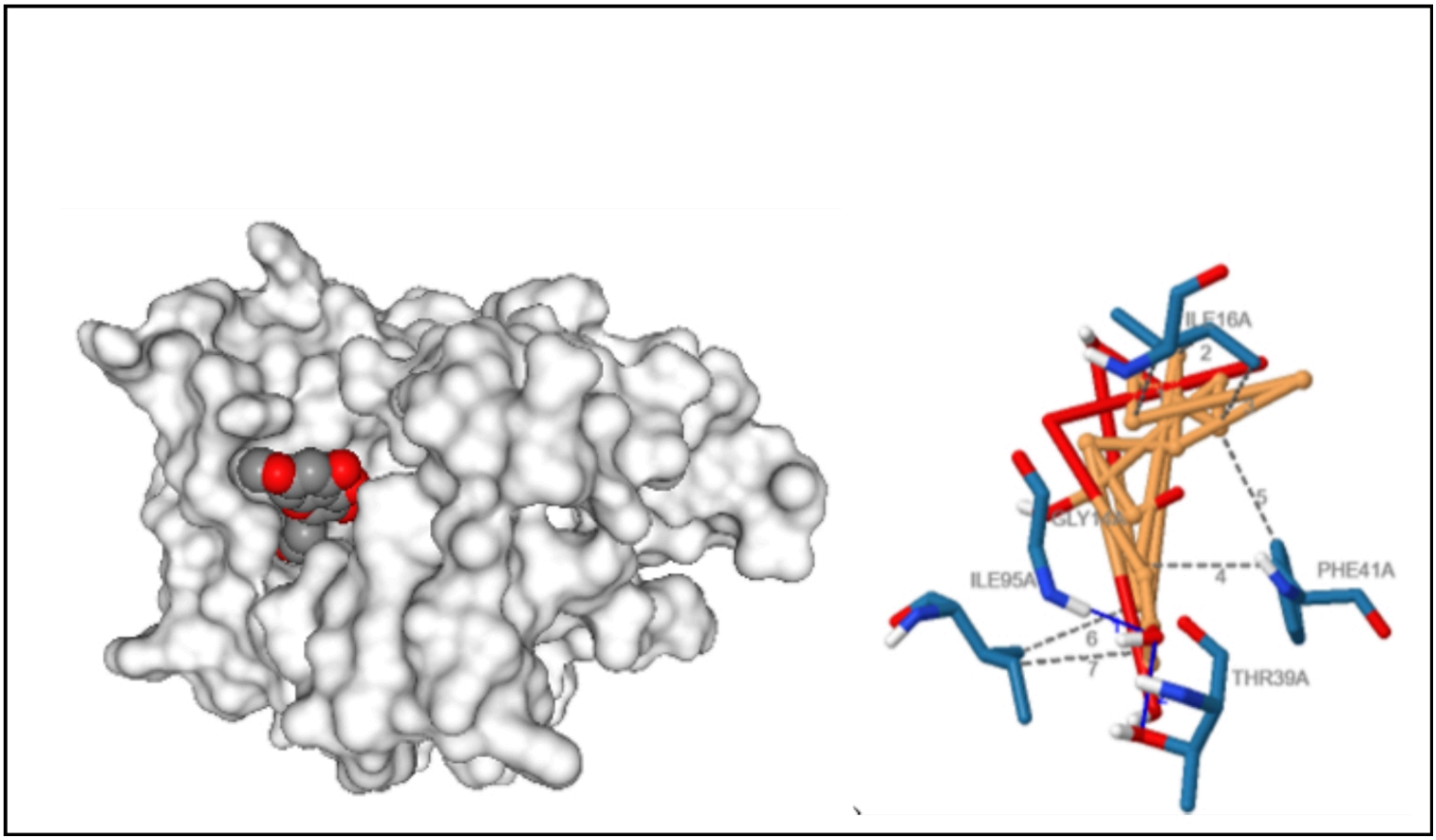

Figure 4

The binding configuration of the bioactive compound derived from *Moringa oleifera*. Rhamnetin in the InhA active site as obtained through molecular docking utilizing AutoDock Vina. Binding interactions were presented in coloured and dotted lines. Grey dotted line – Hydrophobic interaction; Green dashed line – Halogen bond; Green dotted line – Pi stacking; Blue dashed line – Hydrogen bond.

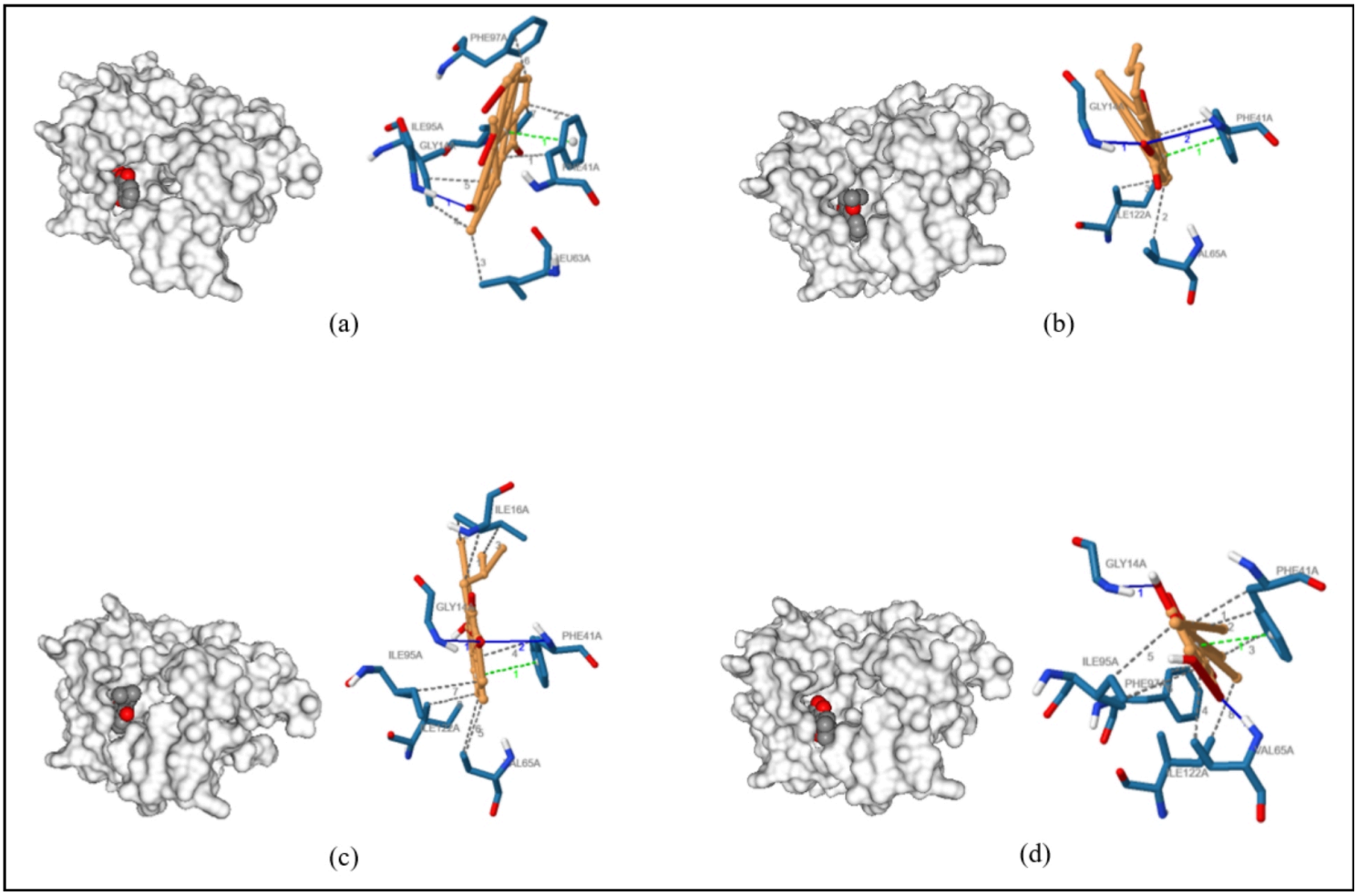

Figure 5

The binding configuration of bioactive compounds derived from *Newbouldia laevis*. (a) Napabucasin, (b) Beta-Lapachone, (c) Lapachol and (d) 5,7-Dihydroxydehydroiso-α-lapachone in the InhA active as obtained through molecular docking utilizing AutoDock Vina. Binding interactions were presented in coloured and dotted lines. Grey dotted line –Hydrophobic interaction; Green dotted line – Pi stacking; Blue dashed line – Hydrogen bond.

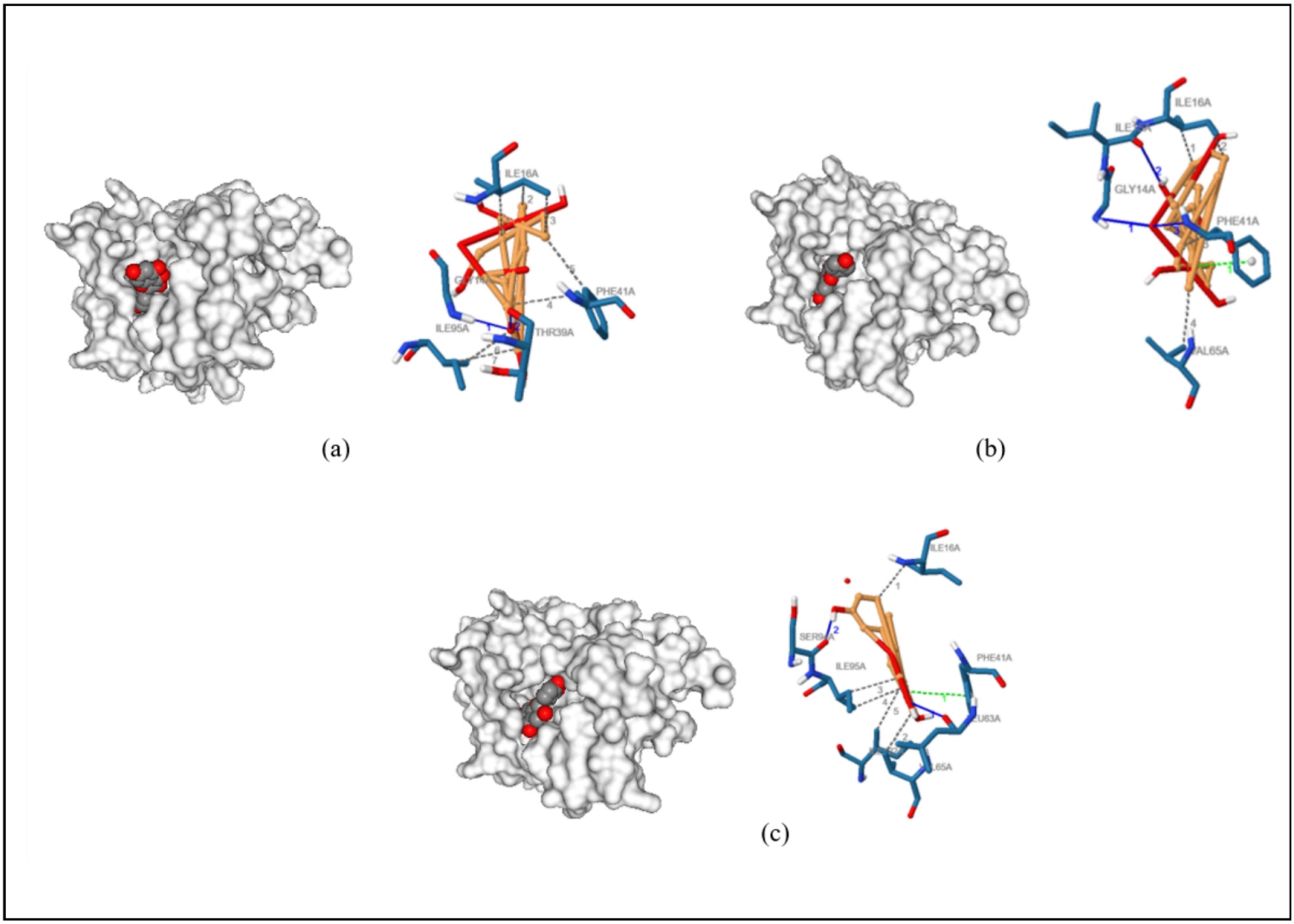

Figure 6

The binding configuration of bioactive compounds derived from *Ocimum gratissimum*. (a) Quercetin, (b) Kaempferol and (c) Catechin in the InhA active site as obtained through molecular docking utilizing AutoDock Vina. Binding interactions were presented in coloured and dotted lines. Grey dotted line – Hydrophobic interaction; Green dotted line – Pi stacking; Blue dashed line – Hydrogen bond.

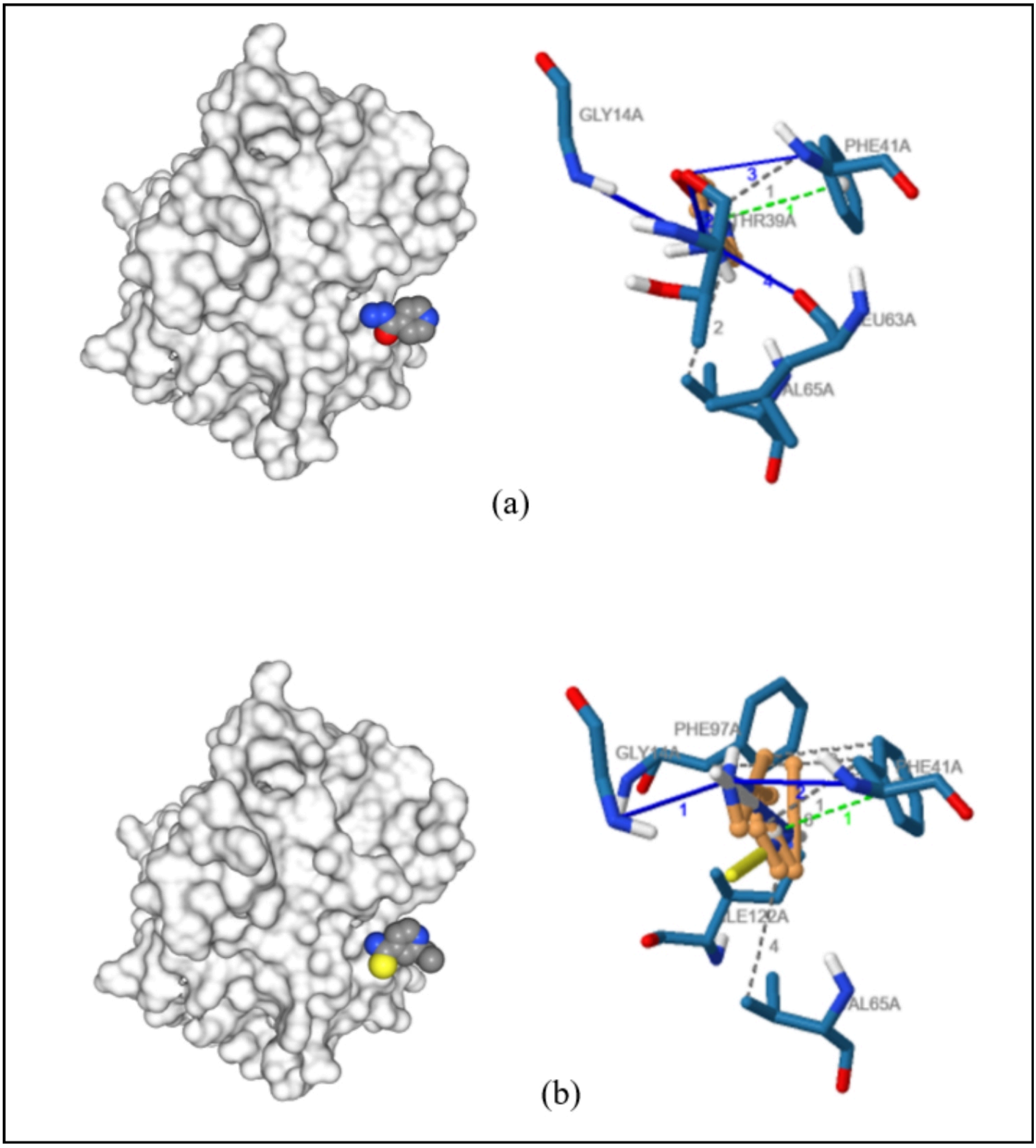

Figure 7

The binding configuration of control drugs. (a) Isoniazid and (b) Ethionamide in the InhA active site as obtained through molecular docking utilizing AutoDock Vina. Binding interactions were presented in coloured and dotted lines. Grey dotted line –Hydrophobic interaction; Green dotted line – Pi stacking; Blue dashed line – Hydrogen bond.

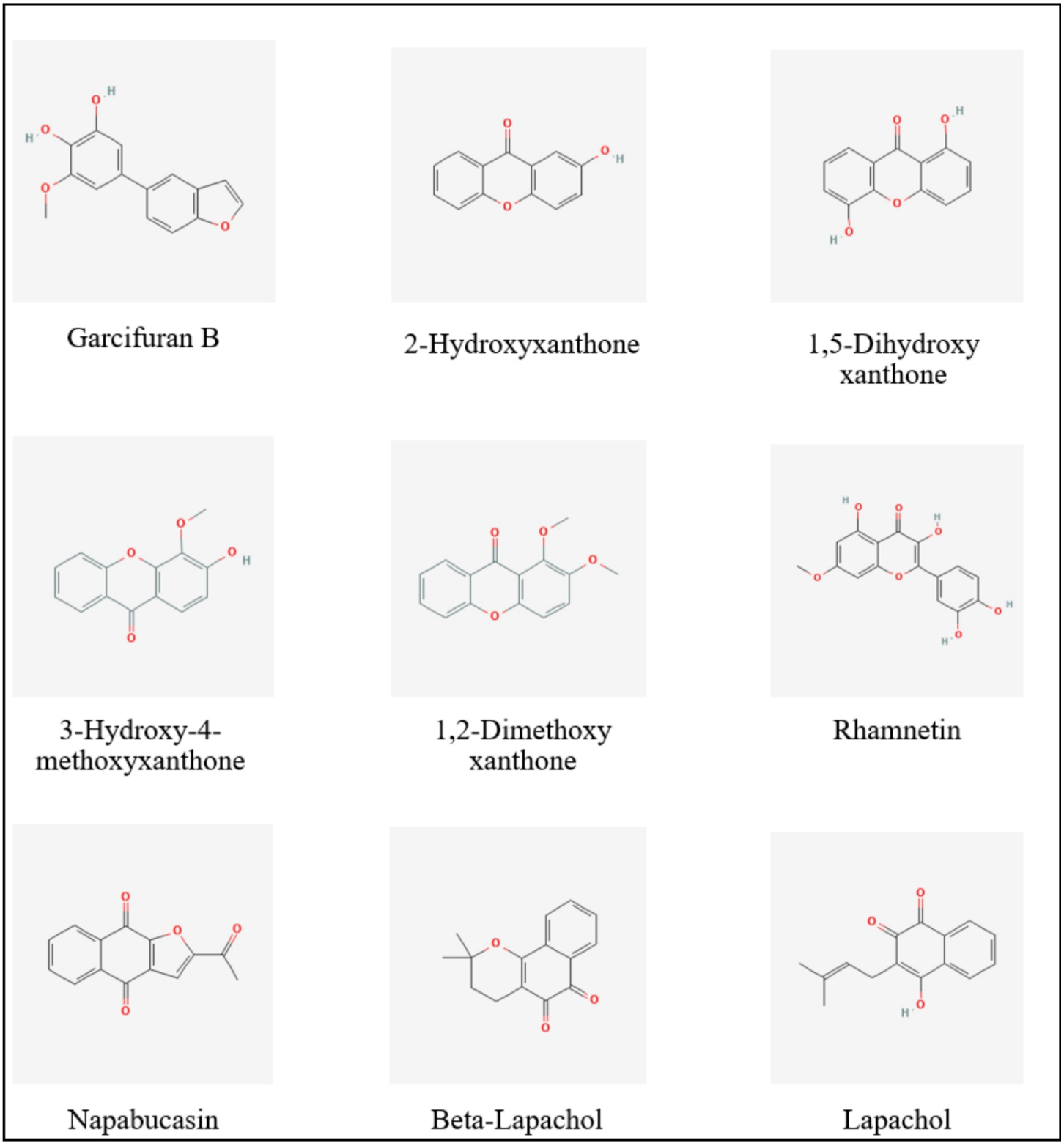

Figure 8

2D structure of bioactive compounds (Adopted from Pubchem)

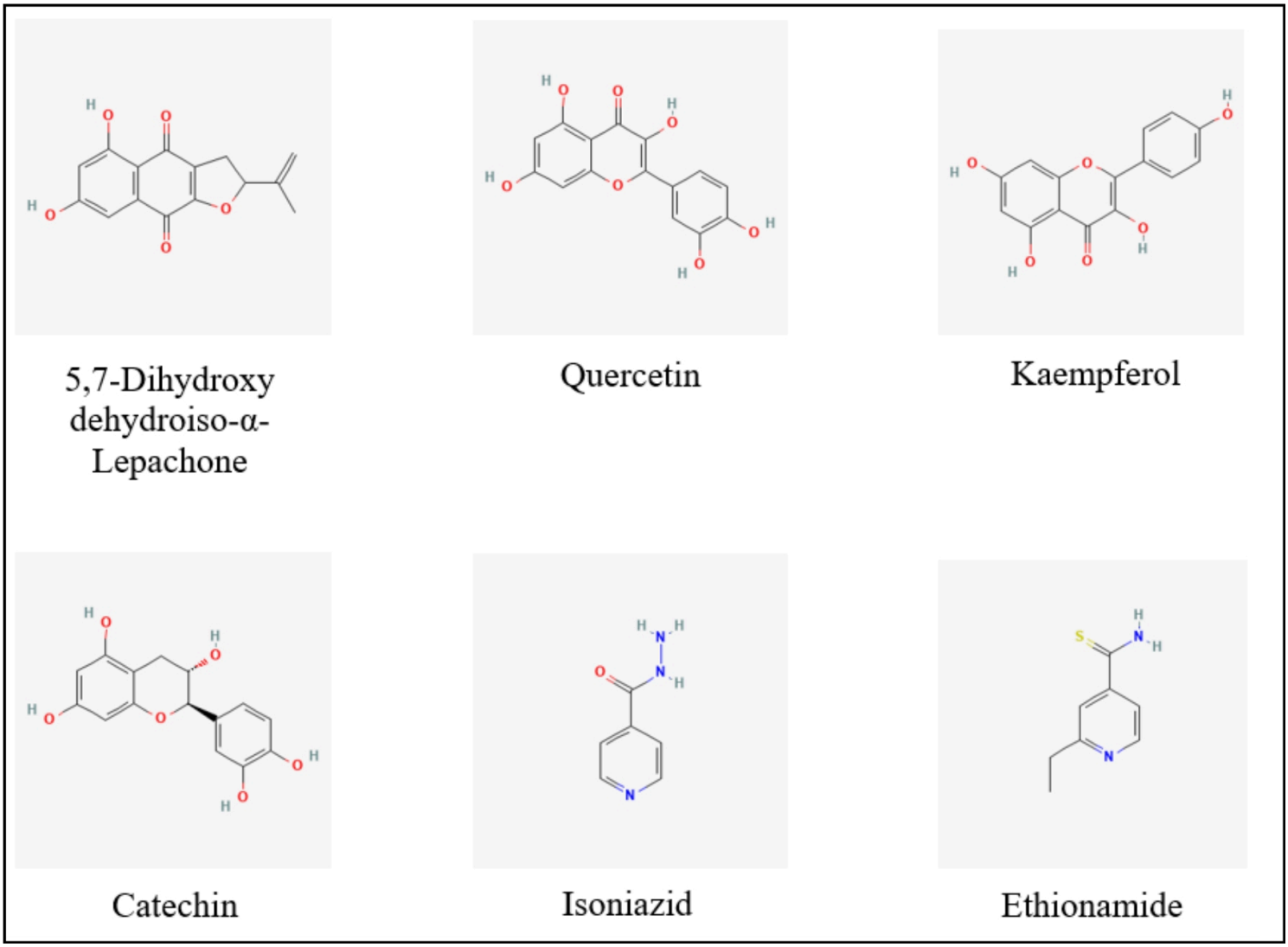

Figure 9

2D structure of bioactive compounds and control drugs (Adopted from Pubchem)

Supplementary Files

This is a list of supplementary files associated with this preprint. Click to download.

- Table5.docx